Author Manuscript

Author Manuscript

Author Manuscript

Author Manuscript

HHS Public Access

Author manuscript

J Physiol. Author manuscript; available in PMC 2022 November 01.

Published in final edited form as:

J Physiol. 2021 November ; 599(22): 4973–4989. doi:10.1113/JP281975.

Nitric oxide synthase inhibition in healthy adults reduces regional and total cerebral macrovascular blood flow and microvascular perfusion

Katrina J Carter[1], **Aaron T Ward**[1], **J Mikhail Kellawan**[6], **Marlowe W Eldridge**[4], **Awni Al-Subu**[4], **Benjamin J Walker**[5], **Jeffrey W Lee**[5], **Oliver Wieben**[2,3], **William G Schrage**[1]

[1]Department of Kinesiology, University of Wisconsin – Madison, WI, USA,

[2]Department of Medical Physics, University of Wisconsin – Madison, WI, USA,

[3]Department of Radiology, University of Wisconsin – Madison, WI, USA,

[4]Department of Pediatrics, University of Wisconsin – Madison, WI, USA,

[5]Department of Anesthesiology, University of Wisconsin – Madison, WI, USA,

[6]Department of Health and Exercise Science, University of Oklahoma, Norman, OK, USA.

Abstract

The importance of nitric oxide (NO) in regulating cerebral blood flow (CBF) remains unresolved, due in part to methodological approaches, which lack comprehensive assessment of both global and regional effects. Importantly, NO synthase (NOS) expression and activity appear greater in some anterior brain regions, suggesting region-specific NOS influence on CBF. We hypothesized that NO contributes to basal CBF in healthy adults, in a regionally distinct pattern that predominates in the anterior circulation. 14 healthy adults (7 females; 24±5 years) underwent two magnetic resonance imaging (MRI) study visits with saline (placebo) or the NOS inhibitor, L-NMMA, administered in a randomized, single-blind approach. 4D Flow MRI quantified total and regional macrovascular CBF, whereas arterial spin labeling (ASL) MRI quantified total and regional microvascular perfusion. L-NMMA (or volume-matched saline) was infused intravenously for 5 minutes prior to imaging. L-NMMA reduced CBF (L-NMMA: 722±100 vs. placebo: 771±121 mL/min, p = 0.01) with similar relative reductions (5–7%) in anterior and posterior cerebral circulations, due in part to reduced cross sectional area of 9 of 11 large cerebral arteries. Global microvascular perfusion (ASL) was reduced by L-NMMA (L-NMMA: 42±7 vs. placebo: 47±8 mL/100g/min, p = 0.02), with 7–11% reductions in both hemispheres of frontal, parietal, and temporal lobes, and in the left occipital lobe. We conclude NO contributes to macrovascular and microvascular regulation including larger artery resting diameter. Contrary to

Bruno Balke Biodynamics Laboratory, Department of Kinesiology, University of Wisconsin-Madison, 1300 University Avenue, Madison, WI 53706

Authors' Contributions

Author Contributions: Conceptualization, M.E., O.W., W.G.S,; Data Acquisition and Interpretation, K.J.C., A.T.W., J.M.K., M.E., A.A., B.J.W., J.W. L., O.W., and W.G.S; Writing—original draft preparation, K.J.C., A.T.W., J.M.K, M.E., A.A., B.J.W., J.W. L., O.W., and W.G.S; Writing—review and editing, K.J.C., A.T.W., J.M.K., M.E., A.A., B.J.W., J.W. L., O.W., and W.G.S.; Supervision, M.E. O.W., and W.G.S.

Disclosure

Dr. Al-Subu (AA) has a consulting agreement with Edwards Lifesciences LLC. Other authors declare no conflicts of interest.

Author Manuscript Author Manuscript Author Manuscript Author Manuscript

our hypothesis, the influence of NO on cerebral perfusion appears regionally uniform in healthy young adults.

Graphical Abstract

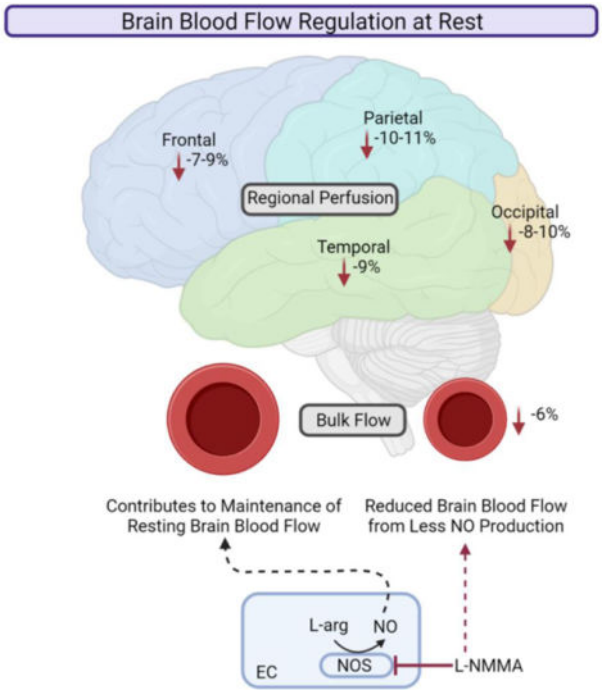

EC, endothelial cell; L-arg, L-arginine; L-NMMA, N^G-monomethyl-L-arginine; NO, nitric oxide; NOS, nitric oxide synthase. NO contributes to the maintenance of resting brain blood flow in humans. Inhibition of nitric oxide synthase by L-NMMA in endothelial cells leads to reduced bulk flow and regional perfusion.

Introduction

Adequate blood flow to the brain is key to support the complex processes crucial for daily life. Conversely, diminished basal cerebral blood flow (CBF) is linked to chronic disability (Martin *et al.* 2002; O'Brien *et al.* 2003), lower cognitive function (Pohjasvaara *et al.* 1998, O'Brien *et al.* 2003; Reitz *et al.* 2008; Kitagawa *et al.* 2009; Wolters *et al.* 2017; Leeuwis *et al.* 2017), lower quality of life (O'Brien *et al.* 2003; Dabrowska-Bender *et al.* 2017) and is a key characteristic of several neurological disorders (Johnson *et al.* 2005; Dai *et al.* 2009; Kitagawa *et al.* 2009; Chao *et al.* 2010; Bangen *et al.* 2012; Binnewijzend *et al.* 2013; Binnewijzend *et al.* 2016; Love and Miners, 2016; Gao 2013), which are the 2nd leading cause of mortality worldwide (Feigin *et al.* 2019). Lower basal CBF has been demonstrated in older adults (Bangen *et al.* 2003; Asllani *et al.* 2009; Lee *et al.* 2009; Chen *et al.* 2011; Bangen *et al.* 2012; Wagner *et al.* 2012, Amiri *et al.* 2014), adults with insulin resistance (Harrell *et al.* 2012; Rusinek *et al.* 2015; Hoschdeit *et al.* 2017; Bangen *et al.* 2018), cardiovascular disease (Muller *et al.* 2012; Roy *et al.* 2017; Iordanova *et al.* 2017; Leeuwis *et al.* 2020), and cerebrovascular disease (Johnson *et al.* 2005; Dai et al. 2009; Kitagawa *et*

Author Manuscript Author Manuscript Author Manuscript Author Manuscript

al. 2009; Chao *et al.* 2010; Bangen *et al.* 2012; Binnewijzend *et al.* 2013; Binnewijzend *et al.* 2016; Love and Miners, 2016; Gao *et al.* 2013). Reduced basal CBF suggests a change or loss in mechanisms responsible for resting CBF control, but the predominant mechanisms regulating CBF in health are not clearly delineated.

Basal CBF appears regulated by multiple, redundant signaling pathways including cyclooxygenase (COX), endothelial-derived hyperpolarizing factor (EDHF), and nitric oxide synthase (NOS). Indeed, studies have demonstrated inhibition of COX with indomethacin decreases middle cerebral artery velocity (MCAv) from 25–41% (Fan *et al.* 2011; Barnes *et al.* 2012; Harrell *et al.* 2014; Lewis *et al.* 2014; Peltonen *et al.* 2015; Hartley *et al.* 2016; Hoiland *et al.* 2016), and Kellawan *et al.* observed an ~44±5% decrease in resting total CBF (2020). These studies indicate a prominent role for COX signaling in regulating resting CBF but suggest other signaling pathways are unresolved. Animal studies demonstrate a minor role for EDHF in regulating CBF through major cerebral vessels compared to the cerebral microcirculation (Shimokawa *et al.* 1996; Urakami-Harasawa *et al.* 1997; Luksha *et al.* 2009; Jiang *et al.* 2016). To date, there is currently no safe way to assess EDHF in the human cerebral circulation. Finally, basal NOS activity is another mechanism implicated in the regulation of resting CBF.

While the role of NOS in maintaining resting blood flow is established in the peripheral circulation (Gardiner *et al.* 1990; Imig *et al.* 1993, Lefroy *et al.* 1993; Huang *et al.* 1995; Shesely *et al.* 1996; Duffy *et al.* 1999; Heinonen *et al.* 2011; Heinonen *et al.* 2017; Heinonen *et al.* 2018), studies of the cerebral circulation report contradictory findings. For example, inhibition of NOS using N^G-monomethyl-L-arginine (L-NMMA) decreased CBF through a single internal carotid artery by 16% (White *et al.* 1998) and reduced global CBF by 20% (White *et al.* 1999). Conversely, other studies have found no effect of NOS inhibition (Schemetterer *et al.* 1997; Van Mil *et al.* 2002; Lassen *et al.* 2003; Lassen *et al.* 2003; Kamper *et al.* 2004; Ide *et al.* 2007; Hoiland *et al.* 2020). One possible explanation for this controversy is pressor response to NOS inhibition confounds data interpretation. For example, blood flow vs. vascular conductance may lead to different conclusions. Another reason for discrepant findings may be differential techniques as most studies that used transcranial Doppler ultrasound (TCD) found no change in CBF with NOS inhibition except for one (Kiss *et al.* 1999) and MRI studies report mixed results. To date, only three studies (White *et al.* 1999; Joshi *et al.* 2000; Lassen *et al.* 2004) have investigated the contributions of NOS to regional CBF, without comprehensive assessment of global and regional CBF. White et al. investigated regional CBF to the bilateral frontal, occipital, and temporal lobes and found CBF was reduced only in the right frontal lobe during NOS inhibition (White *et al.* 1999). Joshi *et al.* (2000) found a 13–20% decrease in regional CBF through the MCA territory during NOS inhibition but did not explore the posterior circulation. Lassen *et al.* (2004) found a 6.8% reduction in CBF through the MCA distribution during NOS inhibition as well as decreased perfusion in the left MCA territory and bilateral ACA territories. A recent paper in humans (O'Gallagher *et al.* 2020) demonstrated a 4% decrease in global CBF as well as region-specific reductions in the right hippocampus, parahippocampal gyrus, and medial temporal lobe using a neuronal NOS (nNOS) specific inhibitor. Importantly data from human and animal studies suggest nNOS and endothelial NOS (eNOS) expression and/or activity varies by brain region (Kovach *et al.* 1992; Pelligrino *et al.* 1993; Northington

Author Manuscript Author Manuscript Author Manuscript Author Manuscript

et al. 1997; Blum-Degen *et al.* 1999; Liu *et al.* 2003). Conceptually, lower CBF in the anterior circulation of during neurological disease progression (Johnson *et al.* 2005; Dai *et al.* 2009; Okonkwo *et al.* 2014) may be explained by a larger anterior influence of NOS. Therefore, it is important to determine whether NOS impacts CBF regionally as well as globally in healthy populations to better understand cerebrovascular pathologies linked to reduced CBF.

Given the controversy surrounding NOS in regulating CBF and the lack of detailed knowledge on potential regional differences in NOS control, the purpose of our study was to quantify global and regional CBF effects of NOS inhibition at the macrovascular and microvascular levels using complementary MRI approaches. We hypothesized that: 1) NO is responsible, in part, for regulating basal CBF in healthy adults; and 2) NOS plays a larger role in regulating basal CBF in anterior versus posterior brain regions.

Methods

Subjects

Fourteen young volunteers participated in the study (7 females, 24±5 years). Written informed consent was obtained before study participation. All procedures conformed to the standards set forth by the Declaration of Helsinki, including registration in the ClinicalTrials.gov database (ClinicalTrials.gov ID: NCT02936687) and were approved by the University of Wisconsin-Madison Health Sciences Institutional Review Board.

Subjects performed an initial screening visit to determine eligibility that included a health history questionnaire, physical activity questionnaire, and MRI safety questionnaire. All subjects were healthy 18–45 years old, sedentary (≤ 90 minutes vigorous exercise per week), free of overt disease and not currently taking any cardiovascular or metabolic medication. Waist circumference, hip circumference, height, and weight were measured, and body mass index (BMI, kg/m^2) was calculated. Brachial artery blood pressure was measured in triplicate using an automated sphygmomanometer (Datex Ohmeda) and the lowest of three blood pressure readings was used to assess eligibility. A fasted (≥ 10 hours) venous blood sample was obtained, and plasma glucose and lipids were measured (Table 1). Exclusion criteria included smoking, overweight/obesity (BMI > 25), blood pressure > 125/80 mmHg, fasting glucose > 100 mg/dl, LDL > 130 mg/dl, triglycerides > 150 mg/dL, or contraindication for MRI. Women were not pregnant or lactating and were studied during the early follicular phase of the menstrual cycle (cycle days 1–5) or low hormone phase of birth control (self-report) except for one female subject who was studied outside cycle days 1–5.

Study visits

Subjects were instructed to report to the laboratory on all study days having fasted for ≥ 10 hours and abstained from vigorous exercise, alcohol, caffeine, and non-steroidal anti-inflammatory drugs for ≥ 24 hours.

Author Manuscript Author Manuscript Author Manuscript Author Manuscript

Instrumentation

Subjects completed two MRI study visits in a randomized, counter-balanced, single-blinded, placebo-controlled design separated by at least 24 hours. MRI scanning was performed using a clinical 3 Tesla MRI system (Discovery MR750, GE Healthcare, Waukesha, WI, USA) and a 32-channel head coil (n = 9) or a 48-channel head coil (n = 5). A study team member visually monitored heart rate (HR; pulse oximeter), arterial oxygen saturation (SpO_2; pulse oximeter), and breath-by-breath end-tidal CO_2 ($ETCO_2$; capnography through nasal cannula) for data stability as well as subject safety. Systolic, diastolic, and mean blood pressure (MABP;automated sphygmomanometer) and hemodynamics (HR, SpO_2, $ETCO_2$) were recorded ~5 minutes into structural scanning and after conclusion of MRI imaging with an MRI compatible system (Fig 1; Medrad Veris MR Vital Signs Patient Monitor, Bayer Healthcare, Whippany, NJ, USA).The exception was the measurement of HR during the PCVIPR scan, which was averaged over the scan period (~5.5 min).

Experimental Protocol (Figure 1)

Subjects reported to the MRI facility and an intravenous (IV) catheter was placed in the antecubital fossa. Subjects then underwent baseline structural scanning for ~15 minutes. Structural scans included: T1-weighted image set, T2-weighted image set, and a 3D Time-of-Flight angiogram of the Circle of Willis. Baseline heart rate, $ETCO_2$ and blood pressure were measured. Next, the non-selective NOS inhibitor N^G-monomethyl-L-arginine (L-NMMA; Bachem) was administered intravenously at 0.6 mg/kg/min for 5 minutes followed by a maintenance infusion at 1 mg/kg/min for 10–11 minutes (during MRI scanning) to determine the effect of NOS inhibition on basal CBF. This dose was based on work by White et. al. (1998) demonstrating ~12% decrease in internal carotid artery flow and that a higher dose increased blood pressure and decreased heart rate while only modestly reducing internal carotid artery flow further (~16%). Placebo (saline) infusion was determined using the same formula for L-NMMA infusion and was infused at the same rate and quantity as during the subject's L-NMMA visit. One male subject was enrolled in a different experimental arm of the study and received a lactose (435.53 mg) pill for their placebo visit for comparison to the drug given in that arm. Blinding procedures were maintained for this participant. The mean dose of L-NMMA was 200±24 mg.

4-Dimensional Flow Magnetic Resonance Imaging (PC VIPR)

Phase-contrast vastly undersampled isotropic projection reconstruction (PC VIPR) was used to obtain 4D flow MRI measurements and quantify blood flow concurrently in eleven separate cerebral conduit arteries. PC VIPR (Gu *et al.* 2005; Johnson *et al.* 2008) is a validated MRI sequence (Schrauben *et al.* 2015; Vikner *et al.* 2020) to simultaneously assess cerebrovascular flow and vessel lumens in multiple vessels and used in various applications, including Alzheimer's Disease (Rivera-Rivera *et al. 2016*), insulin resistance (Hoschdeit *et al.* 2017), and hypoxia challenges (Kellawan *et al.* 2017). The following scan parameters were utilized: imaging volume = 22 × 22 × 22 cm^3, acquired isotropic spatial resolution = (0.69 mm^3), scan time = 5 min 38 seconds, velocity encoding (Venc) = 100 cm/s, flip angle = 8^o, repetition time TR/echo time TE = 6.7/2.8 ms (20 reconstructed cardiac time frames using retrospective cardiac gating and temporal view sharing) (Liu *et al.* 2013).

Author Manuscript Author Manuscript Author Manuscript Author Manuscript

Pseudo-Continuous Arterial Spin Labeling (pcASL)

Cerebral perfusion was assessed using a background-suppressed pseudo-continuous ASL sequence (pcASL). The pcASL sequence featured a 3D fast spin-echo spiral readout utilizing a stack of variable-density 5 ms readout and eight interleaves. Scan parameters were: TR = 4.9 ms; TE = 10.5 ms; FOV = 240 mm; slice thickness = 4 mm no gap; matrix size = 128 × 128; number of excitations (NEX)=3; and labeling RF amplitude = 0.24 mG. The post-labeling delay was 2025 ms. During the same imaging sequence / image slab location as the pcASL, we acquired a fluid-suppressed proton density (PD) scan but without RF labeling preparation. This scan was used for cerebral perfusion flow and image registration.

Data Processing

4D flow data was processed using custom in-house centerline processing software developed in Matlab (Matlab, The Mathworks, Natick, MA, USA), which provides a reliable measurement of cerebral artery blood flow (Schrauben *et al.* 2015). Centerline processing software segments individual vessels in a plane perpendicular to the vessel path, one voxel in width (0.69 mm). At each voxel plane, multiple measurements including time averaged velocity, cross sectional area (CSA), and flow measures for the vessel are collected. For each vessel segment, three to five consecutive cross sections were analyzed and averaged for measures of flow, velocity, and CSA. 11 cerebral conduit arteries were assessed: left and right internal carotid arteries (L-ICA, R-ICA), left and right middle cerebral arteries (L-MCA, R-MCA), left and right anterior cerebral arteries (L-ACA, R-ACA), basilar (BA), left and right vertebral arteries (L-VA, R-VA), and left and right posterior cerebral arteries (L-PCA, R-PCA). To maintain consistency in data analysis and acquire vessel regions with laminar flow, the following locations served as standard sites for data collection: ICA was measured in the straight portion of the C4 segment (Bouthillie *et al.* 1996); ACA and MCA were measured 4–5 mm from their junction with the ICA (A1 and M1 segments, respectively), VA was measured 4–5 mm from the junction with the BA; BA was measured 4–7 mm from the junction with the VA; and PCA was measured 4–5 mm from the junction with the BA. Total CBF was calculated as the sum of the L-ICA, R-ICA, and BA. Total anterior CBF was calculated as the sum of the L-ICA and R-ICA. Total posterior CBF was represented by CBF through the BA.

Cerebral pcASL perfusion images were processed using AFNI, SPM (version 12), and FSL (Bangen *et al.* 2012; Binnewijzend *et al.* 2013; Binnewijzend *et al.* 2016; Hoschdiet *et al.* 2016). First, a set of DICOM images was generated from pcASL CBF weighted images (quantitative CBF image) and PD weighted reference images (PD image) using AFNI. SPM was used to segment gray matter from the T1-weighted images, which was then smoothed using an 8 mm full-width at half-maximum Gaussian kernel and co-registered to the quantitative ASL data (Hoschdeit *et al.* 2016). The co-registered ASL images were normalized to subject head space and a global cerebral perfusion value was calculated using FSL. Cerebral perfusion for bilateral frontal lobe, occipital lobe, parietal lobe, and temporal lobe was determined using FSL. Cerebral perfusion for the pooled vascular territories and bilateral MCA territories, ACA territories, and PCA territories were also determined using FSL.

Author Manuscript Author Manuscript Author Manuscript Author Manuscript

Statistical Analysis

All data are expressed as mean ± standard deviation (SD). R (R Foundation for Statistical Computing, Vienna, Austria) was used for statistical analysis. The main outcome variable was the resting CBF response to NOS inhibition. To assess the contribution of NOS to basal CBF comprehensively, data were expressed as an absolute change in CBF (ΔCBF) and a percent change in CBF (%ΔCBF) from placebo. Region-specific contribution of NOS was determined by calculating total, anterior, and posterior CBF. The basal effect of L-NMMA on resting total and regional (anterior and posterior) CBF was determined with paired t-tests (placebo vs. L-NMMA). A Bonferroni correction was used to determine significance when multiple comparisons were made. Due to technical difficulties, we were unable to obtain $ETCO_2$ measurements for all participants at all timepoints. Importantly, all subjects demonstrated normal levels during their other study visits and the randomization should minimize this impact; however, it is important to note that an $ETCO_2$ value outside the normal range heavily influences CBF (Hoiland *et al.* 2020). Therefore, a general linear mixed effects model with random effects for subjects was used to assess the available $ETCO_2$ data. One sample *t* tests were used to determine if basal changes in CBF with L-NMMA were less than zero. Significance of systemic hemodynamic variables in response to treatment (NOS inhibition) were determined with paired t-tests. Effect size was determined by calculating Cohen's d using means and standard deviations of the two conditions (placebo vs. L-NMMA) according to the following equation: Cohen's $d = M_1 - M_2 \div \sqrt{[(\sigma_1^2 + \sigma_2^2) \div 2]}$, where M_1 is the mean for the placebo condition, M_2 is the mean for the L-NMMA condition, σ_1 is the standard deviation for the placebo condition, and σ_2 is the standard deviation for the L-NMMA condition.

Results

Subjects.

Subject characteristics are summarized in Table 1. Overall, subjects were normal weight, young, displayed healthy blood values and were free of disease. All subjects completed both study visits.

Systemic hemodynamics.

Baseline heart rate, systolic blood pressure, diastolic blood pressure, MABP, and $ETCO_2$ are summarized in Table 2. During MRI scanning, heart rate decreased 8±3 BPM ($P < 0.001$; Cohen's $d = 2.6$; −14±5%) from baseline with L-NMMA and 4±5 BPM ($P = 0.001$; Cohen's $d = 0.9$; −6±7%) from baseline with placebo, and the relative change in heart rate from baseline to MRI scanning (post-drug infusion) was greater with L-NMMA vs. placebo ($P = 0.001$; Cohen's $d = 1.3$). Systolic blood pressure ($P = 0.013$; Cohen's $d = 0.4$), and diastolic blood pressure ($P = 0.022$; Cohen's $d = 0.4$) and MABP ($P = 0.009$; Cohen's $d = 0.5$) were elevated post-scan with L-NMMA (Table 2). $ETCO_2$ was not different by time (baseline vs. post-scan; $P = 0.166$) or condition (placebo vs. L-NMMA; $P = 0.911$) nor was there a significant interaction ($P = 0.594$). These results were not altered when the female who was studied outside of follicular days 1–5 was removed from the dataset.

Author Manuscript Author Manuscript Author Manuscript Author Manuscript

Total and regional macrovascular blood flow.

Macrovascular flow and vessel-specific cerebrovascular responses are summarized in Figures 2 and 3 and Tables 3 and 4. Total CBF was lower with L-NMMA when compared to placebo (Table 3; Fig 2 and 3; P = 0.011; Cohen's d = 0.4). The absolute difference in total CBF with L-NMMA infusion was −49±64 mL/min (Table 3; P = 0.007; Cohen's d = 0.8); a relative decrease in total CBF of 6±8% (Figure 3A; Table 3; P = 0.012; Cohen's d = 0.7). Further, L-NMMA lowered anterior CBF 35±51 mL/min (Table 3; P = 0.013; Cohen's d = 0.7); a relative decrease in anterior CBF of 5±9% (Figure 3B; P = 0.024; Cohen's d = 0.6). Similarly, Posterior CBF was lowered by L-NMMA ~14±18 mL/min (Table 3; P = 0.006; Cohen's d = 0.8) which constitutes a ~7±9% decrease (Fig 3C; P = 0.005; Cohen's d = 0.8). When comparing changes in CBF following L-NMMA infusion between the anterior and posterior circulations, the relative change in CBF was not different (P = 0.228).

Blood vessel structural and hemodynamic characteristics.

To help interpret the effects of NOS inhibition on cerebral blood flow, structural and hemodynamic characteristics of the 11 major cerebral conduit arteries were analyzed. CBF through the L-ICA, R-ICA, L-VA, R-VA, BA, and L-PCA were lower with L-NMMA treatment compared to placebo (Table 4). L-NMMA also lowered cross sectional area in 9 of the 11 large cerebral arteries examined: R-ICA, L-MCA, R-MCA, L-ACA, R-ACA, L-VA, R-VA, BA, and R-PCA (Table 4). Conversely, the mean blood velocity was similar in all blood vessels.

Global and regional microvascular blood flow.

Microvascular flow data are summarized in Table 5 and Figure 4. To explore the role of NOS inhibition on microvascular blood flow in a region-specific manner, we determined total and regional cerebral perfusion using ASL MRI imaging. Perfusion was normalized to gray matter volume, which was not different between study days (L-NMMA: 796±63 vs placebo: 796±70 mL, P = 0.970). L-NMMA reduced total perfusion by 5±7 mL/100g/min, a relative decrease of 10±14% (Table 5; Figure 4A; P = 0.009). Regionally, perfusion was lower in the left and right frontal (P = 0.024, Cohen's d = 0.5; P = 0.012, Cohen's d = 0.7), left occipital (P = 0.022, Cohen's d = 0.6), left and right parietal (P = 0.004, Cohen's d = 0.7; P = 0.018, Cohen's d = 0.7), and left and right temporal (P = 0.005, Cohen's d = 0.6; P = 0.003, Cohen's d = 0.6) lobes (Figure 4; Table 5) with L-NMMA. Relative decreases in perfusion were observed regionally in the left and right frontal, left occipital, left and right parietal, and left and right temporal lobes (Table 5).

Exploratory analysis of vascular territory perfusion.

We also explored changes in perfusion through brain territories typically served by well-established arterial networks. The perfusion through pooled vascular territories was lower with L-NMMA (Table 6; 41±7 mL/100g/min, P = 0.009; Cohen's d = 0.8) compared to placebo (47±8 mL/100g/min). Perfusion was decreased in the right (P = 0.021; Cohen's d = 0.7) and left (P = 0.011; Cohen's d = 0.7) ACA territory, right (P = 0.025; Cohen's d = 0.7) and left (P = 0.025; Cohen's d = 0.6) MCA territory, and right (P = 0.043; Cohen's d = 0.6) and left (P = 0.028; Cohen's d = 0.7) PCA territory with L-NMMA. The

Author Manuscript Author Manuscript Author Manuscript Author Manuscript

absolute change in perfusion following L-NMMA was significantly different for all vascular territories examined and the relative change was significantly different for all vascular territories except the right and left PCA territory (Table 6).

Anatomical variations.

The following anatomical variation was noted: one participant had a R PCA that originated from the R ICA; the R VA was anatomically absent in two participant; one participant was missing the L VA and their R and L PCA was connected to the R ICA and L ICA, respectively, as well as the BA; two participants had a R PCA that connected to the R ICA and BA; one participant had a dominant L VA and the L ACA was anatomically absent; one participant had a R PCA that connected to the R ICA and BA and their L ACA was anatomically absent; one participant had a R and L PCA that was connected to the R ICA and L ICA, respectively, as well as the BA.

Discussion

The aim of this investigation was to examine the contribution of NOS to basal CBF from both macrovascular and microvascular perspectives, on a total and region-specific basis. This systematic approach led to several novel findings: 1) CBF was lower with L-NMMA due to decreases in CBF in major anterior and posterior arteries, 2) CSA was lower with L-NMMA in several major arteries while mean velocity did not change, and 3) global microvascular perfusion was also lower with L-NMMA in most brain regions. These data clearly demonstrate NOS signaling contributes to basal CBF and perfusion and offer a more complete view into total and region-specific contribution of NOS to basal CBF regulation in healthy adults.

Effects of NOS inhibition on basal macrovascular blood flow.

In agreement with our hypothesis, healthy adults exhibited a 6±8% decrease in basal total CBF during L-NMMA infusion (Table 3, Fig 2 and 3). Prior work investigating the impact of NOS inhibition on basal macrovascular CBF reported conflicting results, ranging from no effect to 16% reductions. Of the studies that observed no change in macrovascular CBF after L-NMMA, five used TCD (Schemetterer *et al.* 1997; Lassen *et al.* 2003; Lassen *et al.* 2003; Lassen *et al.* 2004; Ide *et al.* 2007) and two used phase contrast MRI (Van Mil *et al.* 2002; Kamper *et al.* 2004). Interestingly, White *et al.* (1998) detected a 12% decrease in ICA flow with L-NMMA, but no change in CBF velocity through the MCA (TCD). Similarly, recent data from Hoiland *et al.* using TCD of the MCA and PCA found no change in CBF velocity or global CBF (Doppler ultrasound) with intravenous infusion of L-NMMA (5 mg/kg), however they did detect a 6.5% decrease in global cerebrovascular conductance with L-NMMA (Hoiland *et al.* 2020), which supports the current macrovascular findings. Our results are consistent with the findings that NOS inhibition does not change CBF velocity in MCA or PCA and data in Table 4 expand this concept to nearly all major cerebral arteries. Specifically, L-NMMA decreased CSA in MCA, ACA, VA, BA and one ICA (Table 4). Taken together, studies using TCD of MCA or most other large cerebral arteries appear unlikely to detect changes in CBF during NOS inhibition as CBF changes were driven by changes in artery CSA (Table 4).

Author Manuscript Author Manuscript Author Manuscript Author Manuscript

CBF is inherently variable between subjects, and this variability is exemplified by left-right differences in CBF (Table 4). This inherent variability may lend to the disagreement between CBF studies and the L-NMMA effect. For example, Hoiland *et al.* (2020) calculated global CBF as twice the sum of the unilateral ICA blood flow and VA blood flow values, which assumes flow is the same through both ICAs and VAs. This assumption may not hold true as anatomical variation may lead to a dominant ICA or VA and some individuals lack two VA (Friend *et al.* 2021). It is also possible left-right variability response to L-NMMA limits prior consensus, as current data in Table 4 indicate left ICA demonstrates half the decrease in CBF due to L-NMMA compared to the right ICA. Van Mil *et al.* (2002) and Kamper *et al.* (2004) measured CBF using gradient echo phase contrast MRI in both ICAs and the BA during intravenous infusion of L-NMMA, and both studies report infusion of L-NMMA did not affect global CBF. These two studies used comparable doses (3 mg/kg) to White *et al.* (1998) who reported L-NMMA decreased flow in the right ICA by ~12%. Finally, Van Mil *et al.* (2002) and Kamper *et al.* (2004) report total flow (the sum of blood flow through the left and right ICAs and the BA), while White *et al.* (1998) report flow through a single ICA. Without reporting CSA and velocity of each artery, or by not interrogating all cerebral arteries, it is difficult to make conclusions about the regional effects of NOS inhibition on the macrovascular cerebral circulation. Data in Figs 2–3 and Table 4 address these prior research limitations and lead us to the conclude L-NMMA does indeed decrease CBF primarily through reduced CSA, albeit not uniformly at the macrovascular level.

Animal studies (Kovach *et al.* 1992; Northington *et al.* 1997; Liu *et al.* 2003; Campese *et al.* 2007) and one human study (Blum-Degen *et al.* 1999) indicate NOS expression or activity is non-uniform across the brain, demonstrating the need to assess whether CBF control by NOS varies between brain regions. Contrary to our hypothesis, the decrease in total CBF was not preferentially directed toward the anterior circulation (Fig 3). A novel aspect of this study was the ability to assess CBF simultaneously in all major cerebral arteries, rather than previous work in 1–2 single vessels (Schemetterer *et al.* 1997; White *et al.* 1998; Kiss *et al.* 1999; Joshi *et al.* 2000; Lassen *et al.* 2003; Lassen *et al.* 2003; Lassen *et al.* 2004; Ide *et al.* 2007; Hoiland *et al.* 2020). The change in CBF in most arteries was significant, but modest (4–7%, Table 4) indicating other signaling (e.g., cyclooxygenase) provides greater vascular support of basal brain perfusion (Markus *et al.* 1994; Gjedde *et al.* 2005; Barnes *et al.* 2012; Beaudin *et al.* 2014; Harrell *et al.* 2012; Harrell *et al.* 2014; Peltonen *et al.* 2015; Bain *et al.* 2016; Hoiland *et al.* 2016; Peltonen *et al.* 2016; Harrell *et al.* 2019; Kellawan *et al.* 2020; Rocha *et al.* 2020). These more complete macrovascular measures, along with ASL measures (Fig 4) discussed below suggest the functional role of NOS is similar anterior versus posterior in healthy humans despite the potential for differential NOS protein expression profiles (Kovach *et al.* 1992; Northington *et al.* 1997; Blum-Degen *et al.* 1999; Liu *et al.* 2003; Campese *et al.* 2007).

Effects of NOS inhibition on basal microvascular blood flow.

While large cerebral arteries can contribute substantial cerebrovascular resistance (Willie et al. 2014), the microcirculation plays a key role in final determination of meeting metabolic demand due to neurovascular coupling. To address the role of NOS in microcirculation, we measured CBF using ASL, a non-invasive and well-validated MRI technique used to

Author Manuscript Author Manuscript Author Manuscript Author Manuscript

assess blood flow both globally and to specific brain regions. Data summarized in Table 5 and Fig 4 indicate that perfusion is reduced during NOS inhibition. In agreement with our hypothesis, healthy adults exhibited a 10% decrease in basal global perfusion during L-NMMA infusion and a 7–11% decrease in regional perfusion. However, contrary to our hypothesis regional decreases in perfusion during L-NMMA administration did not predominate in anterior regions. The unchanged velocity data in large arteries (Table 4) is consistent with our microvascular findings, but also suggests arterioles of intermediate size are playing a role in NOS regulation of CBF. Unfortunately, this speculation cannot be confirmed because current MRI methods do not allow us to measure CBF in that region of the vascular tree.

Present ASL results do agree with a relatively mild to moderate L-NMMA effect previously reported in the literature. Depending on the protocol, White *et al.* (1999) observed an 11–20% decrease in global perfusion during NOS inhibition, while Joshi *et al.* (2000) observed a 12–20% decrease in global perfusion during NOS inhibition. White *et al.* (1999) used high resolution PET MRI, while Joshi *et al.* (2000) used the ^{133}Xenon injection technique with CBF probes positioned over the MCA distribution to measure changes in perfusion. White et al. used an intravenous bolus infusion of L-NMMA at 10 mg/kg (estimated mean total dose: 853mg), while Joshi *et al.* (2000) used an intraarterial infusion of L-NMMA at 50mg/min for 5 min (total dose: 250mg). Taken together, the range in CBF reductions (11–20%) are likely not due to route or dose of L-NMMA administration. Rather, small sample sizes (n=5–8), middle-aged subjects (45+ years), inclusion of subjects with comorbidities or cerebrovascular malformations, and use of sedation may contribute more to variability in global perfusion changes during NOS inhibition. In fact, Kamper *et al.* (2004) reported an effect of L-NMMA in older but not younger subjects, which appears counterintuitive to most aging literature in peripheral circulations. Current ASL data disagrees with White *et al.* (1999) who reported no effect of NOS inhibition in the right and left frontal, occipital, and temporal lobes, or the right and left motor cortex. The 10–11% reduction in global perfusion (Table 5) is slightly more than Lassen *et al.* (2004) reporting a 6.8% lower perfusion in the right MCA territory as well as the left MCA territory and both ACA territories, although perfusion values and L-NNMA effects of these 3 regions were not reported and likely modest. Taken together, the bulk of prior ASL studies, and present data (Table 5 Fig 4), support the conclusion that NOS is responsible for 7–12% of basal microvascular perfusion depending on region, with many regions demonstrating roughly 11% reductions. Finally, our exploratory analysis of cerebral perfusion to different vascular territories fed by major arteries (Table 6) supports this conclusion, with a 9–10% decrease in cerebral perfusion from L-NMMA in both hemispheres of the MCA, ACA, and PCA territories.

Vessel-Specific Effect of NOS Inhibition—This is the first study to show how the major cerebral arteries of the Circle of Willis are affected during NOS inhibition. Previously, data was limited to CBF changes in a select few cerebral vessels, lacked CSA measures, and provided little insight to whether NOS was affecting downstream resistance arteries or the conduit arteries themselves. Data summarized in Table 4 indicate that cross-sectional area was reduced with NOS inhibition in the basilar artery, right ICA, right PCA, and the right and left MCAs, ACAs, and VAs, while mean blood flow velocity remained

Author Manuscript Author Manuscript Author Manuscript Author Manuscript

unchanged. Despite changes in CSA, CBF only decreased in the basilar artery, left PCA, and right and left ICAs and VAs, while CBF through the MCAs and ACAs remained unaffected. These data suggest that intravenous infusion of 3 mg/kg of L-NMMA over 5 minutes leads to vasoconstriction of the cerebral conduit arteries and the downstream cerebrovasculature. Furthermore, our global and regional perfusion data indicate L-NMMA decreased microvascular CBF (Table 5–6). Unfortunately, current technology limits our ability to determine where these changes are occurring in distal cerebral vessels smaller than ~1.5 mm in diameter.

Experimental Considerations—This study is not without its limitations. First, one female was studied outside of her early follicular phase, but statistical analysis with this female removed did not change any primary outcomes. However, a few secondary outcomes stayed quantitatively similar despite becoming only trending in significance. Specifically, the Δ%CBF in the left frontal lobe became non-significant (with female: −7±15%, p = 0.044 vs. without female: −8±16%, p = 0.054) and the ΔCBF in the right occipital lobe became significant (with female: −5±11 mL/100g/min, p = 0.058 vs. without female: −6±12 mL/100g/min, p = 0.047; Table 5). Similarly, some secondary measures in Table 4 and Table 5 gained or lost significance (indicated by italics) but remained quantitatively similar with trending significance, so her data were included in the analyses. Second, due to technical difficulties we were unable to measure $ETCO_2$ in five participants during baseline placebo (n = 9), four participants during post-scan placebo (n = 10), one participant during baseline L-NMMA (n = 13), and one participant during post-scan L-NMMA (n = 13). Importantly all subjects demonstrated normal levels on their other scan visits and the randomization should minimize this impact; however, it is important to note that an $ETCO_2$ value outside the normal range heavily influences CBF (Hoiland *et al.* 2019). Third, we did not measure blood pressure during infusion of L-NMMA, such that we may have missed a larger pressor effect of L-NMMA (White *et al.* 1998; Schemetterer *et al.* 1997; Kiss *et al.* 1999; White *et al.* 1999; Joshi *et al.* 2000; Lassen *et al.* 2003 Kamper *et al.* 2004; Lassen *et al.* 2004; Ide *et al.* 2007). Along these lines, current results may slightly underestimate NOS contribution, as higher dosing demonstrated up to 20% reductions in CBF (ASL), but the same studies showed subgroups with results similar to current findings. However, the decrease in heart rate (Table 2) and the increased blood pressure post-scanning suggest that we used an adequate dose of L-NMMA to sufficiently inhibit NOS. Fourth, we did not test for an independent effect of elevated MABP; however, previous studies using a blood pressure control (White *et al.* 1998; Joshi *et al.* 2000; Ide *et al.* 2007; Hoiland *et al.* 2020) have shown that elevated MABP alone does not account for the decrease in CBF during NOS inhibition. Fifth, L-NMMA is a non-specific NOS inhibitor. Therefore, we cannot determine which NOS isoforms (eNOS vs. nNOS) play a predominate role in CBF control. Data recently published by O'Gallagher *et al.* demonstrate an ~4% decrease in resting global microvascular CBF with nNOS blockade (2021). This does not completely account for the 10% decrease in global perfusion we report here, which may suggest both nNOS and eNOS play an important role in regulating resting CBF. Sixth, we do not assess the efficacy of NOS inhibition, although bradycardia effects suggest NOS was significantly inhibited. Seventh, we did not perform MRI scanning prior to infusion to determine how placebo or NOS inhibition affects resting CBF, which makes it impossible to assess between-day or within-

Author Manuscript Author Manuscript Author Manuscript Author Manuscript

subject variance in our data; however, 4D flow MRI has demonstrated low (<12%; typically, 6–8%) coefficient of variances for measurements taken at the same scanning facility on different days and good test-retest reliability (r = 0.75–0.94) for CBF (Wen *et al.* 2019). Furthermore, pcASL has also demonstrated good reproducibility (intraclass correlation coefficient <0.6) and low coefficient of variances (<10% when n>6) for measurements taken on different days (Chen *et al.* 2011; Almeida *et al.* 2018). We agree that the L-NMMA effect is within these ranges but given the random treatment order of placebo and L-NMMA, we propose this does not significantly impact interpretation. Finally, the relative importance of NOS signaling on CBF regulation may differ at rest compared to environmental stress (Hoiland *et al.* 2020).

The strengths of this study include a randomized, single-blind crossover design, a larger cohort than most previous CBF studies manipulating NOS signaling, large effect sizes to increase confidence in data interpretation, and rigorously screened healthy young adults (half female) while controlling for age, BMI, and key cardiovascular risk factors. The combined use of non-invasive MRI to assess global and regional macrovascular and microvascular blood flow which provided data on hemodynamic and structural characteristics of 11 major cerebral conduit arteries, led to the most comprehensive study to date on the impact of NOS on global and regional CBF at macro and microvascular levels.

Summary and Conclusion—In conclusion, we show that total macrovascular CBF is reduced with L-NMMA due similar relative decreases (5–6%) in anterior and posterior CBF in healthy adults. Furthermore, both global and regional perfusion is reduced with L-NMMA by ~10%. These data suggest that NOS signaling is key to overall macrovascular and microvascular CBF control in healthy younger adults, with a fairly uniform impact in several brain regions. Future studies should investigate how NOS signaling is impacted in conditions such as aging, insulin resistance, and diabetes or the importance of other signaling pathways such as endothelial-derived hyperpolarizing factors—which play a key role in microcirculatory signaling—on total and regional CBF regulation.

Supplementary Material

Refer to Web version on PubMed Central for supplementary material.

Acknowledgements

We would like to thank all the study participants. We would also like to thank MRI center staff for their assistance with data collection.

Funding

Funding for this project was provided by the American Diabetes Association (ADA1-16-ICTS-099 to WGS). KJC was supported by the UW-Madison Cardiovascular Research Center Grant # 5 T32 HL 7936-18 and the SciMed Graduate Research Scholars Fellowship, Office of Vice Chancellor for Research and Graduate Education at the University of Wisconsin-Madison, with funding from the Wisconsin Alumni Research Foundation and the UW-Madison. ATW is supported by American Heart Association 11PRE7390038.

The project described was supported by the Clinical and Translational Science Award (CTSA) program, through the NIH National Center for Advancing Translational Sciences (NCATS), grant UL1TR002373. The content is solely the responsibility of the authors and does not necessarily represent the official views of the NIH.

Author Manuscript Author Manuscript Author Manuscript Author Manuscript

Biography

Katrina Carter is currently completing her PhD at the University of Wisconsin-Madison under the supervision of Prof. William Schrage. Her broad interests include the impact of extreme environments on human physiology, but her current research focuses on cerebral blood flow regulation in healthy adults and adults with metabolic syndrome and assessing how metabolic syndrome alters mechanisms that regulate CBF. In the future, she hopes to study how space and space travel affect human physiology in preparation for interplanetary exploration.

Data Availability Statement

The data that support the findings of this study are not publicly available due to privacy/ethical restrictions.

References

Almeida JRC, Greenberg T, Lu H, Chase HW, Fournier JC, Cooper CM, Deckersbach T, Adams P, Carmody T, Fava M, Kurian B, McGrath PJ, McInnis MG, Oquendo MA, Parsey R, Weissman M, Trivedi M & Phillips ML (2018). Test-retest reliability of cerebral blood flow in healthy individuals using arterial spin labeling: Findings from the EMBARC study. Magnetic Resonance Imaging 45, 26–33. [PubMed: 28888770]

Amiri M, Pouliot P, Bonnéry C, Leclerc P-O, Desjardins M, Lesage F & Joanette Y (2014). An Exploration of the Effect of Hemodynamic Changes Due to Normal Aging on the fNIRS Response to Semantic Processing of Words. Front Neurol; DOI: 10.3389/fneur.2014.00249.

Bain AR, Ainslie PN, Hoiland RL, Willie CK, MacLeod DB, Madden D, Maslov PZ, Drviš I & Dujić Ž (2016). Role of cerebral blood flow in extreme breath holding. Translational Neuroscience 7, 12–16. [PubMed: 28123816]

Bangen KJ, Restom K, Liu TT, Jak AJ, Wierenga CE, Salmon DP & Bondi MW (2009). Differential age effects on cerebral blood flow and BOLD response to encoding: Associations with cognition and stroke risk. Neurobiology of Aging 30, 1276–1287. [PubMed: 18160181]

Bangen KJ, Restom K, Liu TT, Wierenga CE, Jak AJ, Salmon DP & Bondi MW (2012). Assessment of Alzheimer's Disease Risk with Functional Magnetic Resonance Imaging: An Arterial Spin Labeling Study. Mandal PK. JAD 31, S59–S74. [PubMed: 22531427]

Bangen KJ, Werhane ML, Weigand AJ, Edmonds EC, Delano-Wood L, Thomas KR, Nation DA, Evangelista ND, Clark AL, Liu TT & Bondi MW (2018). Reduced Regional Cerebral Blood Flow Relates to Poorer Cognition in Older Adults With Type 2 Diabetes. Front Aging Neurosci 10, 270. [PubMed: 30250430]

Barnes JN, Schmidt JE, Nicholson WT & Joyner MJ (2012). Cyclooxygenase inhibition abolishes age-related differences in cerebral vasodilator responses to hypercapnia. Journal of Applied Physiology 112, 1884–1890. [PubMed: 22442028]

Beaudin AE, Pun M, Yang C, Nicholl DDM, Steinback CD, Slater DM, Wynne-Edwards KE, Hanly PJ, Ahmed SB & Poulin MJ (2014). Cyclooxygenases 1 and 2 Differentially Regulate Blood Pressure and Cerebrovascular Responses to Acute and Chronic Intermittent Hypoxia: Implications for Sleep Apnea. JAHA; DOI: 10.1161/JAHA.114.000875.

Author Manuscript Author Manuscript Author Manuscript Author Manuscript

Binnewijzend MAA, Benedictus MR, Kuijer JPA, van der Flier WM, Teunissen CE, Prins ND, Wattjes MP, van Berckel BNM, Scheltens P & Barkhof F (2016). Cerebral perfusion in the predementia stages of Alzheimer's disease. Eur Radiol 26, 506–514. [PubMed: 26040647]

Binnewijzend MAA, Kuijer JPA, Benedictus MR, van der Flier WM, Wink AM, Wattjes MP, van Berckel BNM, Scheltens P & Barkhof F (2013). Cerebral Blood Flow Measured with 3D Pseudocontinuous Arterial Spin-labeling MR Imaging in Alzheimer Disease and Mild Cognitive Impairment: A Marker for Disease Severity. Radiology 267, 221–230. [PubMed: 23238159]

Blum-Degen D, Heinemann T, Lan J, Pedersen V, Leblhuber F, Paulus W, Riederer P & Gerlach M (1999). Characterization and regional distribution of nitric oxide synthase in the human brain during normal ageing. Brain Research 834, 128–135. [PubMed: 10407101]

Campese VM, Sindhu RK, Ye S, Bai Y, Vaziri ND & Jabbari B (2007). Regional expression of NO synthase, NAD(P)H oxidase and superoxide dismutase in the rat brain. Brain Research 1134, 27–32. [PubMed: 17196179]

Chao LL, Buckley ST, Kornak J, Schuff N, Madison C, Yaffe K, Miller BL, Kramer JH & Weiner MW (2010). ASL Perfusion MRI Predicts Cognitive Decline and Conversion From MCI to Dementia. Alzheimer Disease & Associated Disorders 24, 19–27. [PubMed: 20220321]

Chen JJ, Rosas HD & Salat DH (2011). Age-associated reductions in cerebral blood flow are independent from regional atrophy. NeuroImage 55, 468–478. [PubMed: 21167947]

Chen Y, Wang DJJ & Detre JA (2011b). Test-retest reliability of arterial spin labeling with common labeling strategies. J Magn Reson Imaging 33, 940–949. [PubMed: 21448961]

Dąbrowska-Bender M, Milewska M, Gołąbek A, Duda-Zalewska A & Staniszewska A (2017). The Impact of Ischemic Cerebral Stroke on the Quality of Life of Patients Based on Clinical, Social, and Psychoemotional Factors. Journal of Stroke and Cerebrovascular Diseases 26, 101–107. [PubMed: 27746082]

Dai W, Lopez OL, Carmichael OT, Becker JT, Kuller LH & Gach HM (2009). Mild Cognitive Impairment and Alzheimer Disease: Patterns of Altered Cerebral Blood Flow at MR Imaging. Radiology 250, 856–866. [PubMed: 19164119]

Duffy SJ, Castle SF, Harper RW & Meredith IT (1999). Contribution of Vasodilator Prostanoids and Nitric Oxide to Resting Flow, Metabolic Vasodilation, and Flow-Mediated Dilation in Human Coronary Circulation. Circulation 100, 1951–1957. [PubMed: 10556220]

Fan J-L, Burgess KR, Thomas KN, Peebles KC, Lucas SJE, Lucas RAI, Cotter JD & Ainslie PN (2011). Influence of indomethacin on the ventilatory and cerebrovascular responsiveness to hypoxia. Eur J Appl Physiol 111, 601–610. [PubMed: 20938783]

Feigin VL et al. (2019). Global, regional, and national burden of neurological disorders, 1990–2016: a systematic analysis for the Global Burden of Disease Study 2016. The Lancet Neurology 18, 459–480. [PubMed: 30879893]

Friend AT, Rogan Matthew, Rossetti GMK, Lawley JS, Mullins PG, Sandoo A, Macdonald JH & Oliver SJ (2021). Bilateral regional extracranial blood flow regulation to hypoxia and unilateral duplex ultrasound measurement error. Exp Physiol EP089196.

Gao Y-Z, Zhang J-J, Liu H, Wu G-Y, Xiong L & Shu M (n.d.). Regional Cerebral Blood Flow and Cerebrovascular Reactivity in Alzheimer's Disease and Vascular Dementia Assessed by Arterial Spin- labeling Magnetic Resonance Imaging. 5.

Gardiner SM, Compton AM, Bennett T, Palmer RM & Moncada S (1990). Control of regional blood flow by endothelium-derived nitric oxide. Hypertension 15, 486–492. [PubMed: 2332239]

Gjedde A, Johannsen P, Cold GE & Østergaard L (2005). Cerebral Metabolic Response to Low Blood Flow: Possible Role of Cytochrome Oxidase Inhibition. J Cereb Blood Flow Metab 25, 1183–1196. [PubMed: 15815583]

Harrell JW, Morgan BJ & Schrage WG (2013). Impaired hypoxic cerebral vasodilation in younger adults with metabolic syndrome. Diabetes and Vascular Disease Research 10, 135–142. [PubMed: 22752659]

Harrell JW, Peltonen GL & Schrage WG (2019). Reactive oxygen species and cyclooxygenase products explain the majority of hypoxic cerebral vasodilation in healthy humans. Acta Physiol; DOI: 10.1111/apha.13288.

Author Manuscript Author Manuscript Author Manuscript Author Manuscript

Harrell JW & Schrage WG (2014). Cyclooxygenase-derived vasoconstriction restrains hypoxia-mediated cerebral vasodilation in young adults with metabolic syndrome. American Journal of Physiology-Heart and Circulatory Physiology 306, H261–H269. [PubMed: 24213610]

Hartley GL, Watson CL, Ainslie PN, Tokuno CD, Greenway MJ, Gabriel DA, O'Leary DD & Cheung SS (2016). Corticospinal excitability is associated with hypocapnia but not changes in cerebral blood flow: Cerebral blood flow and hypocapnia on corticospinal excitability. J Physiol 594, 3423–3437. [PubMed: 26836470]

Heinonen I, Boushel R, Hellsten Y & Kalliokoski K (2018). Regulation of bone blood flow in humans: The role of nitric oxide, prostaglandins, and adenosine. Scand J Med Sci Sports 28, 1552–1558. [PubMed: 29377406]

Heinonen I, Saltin B, Hellsten Y & Kalliokoski KK (2017). The effect of nitric oxide synthase inhibition with and without inhibition of prostaglandins on blood flow in different human skeletal muscles. Eur J Appl Physiol 117, 1175–1180. [PubMed: 28432421]

Hoiland RL, Caldwell HG, Howe CA, Nowak-Flück D, Stacey BS, Bailey DM, Paton JFR, Green DJ, Sekhon MS, Macleod DB & Ainslie PN (2020). Nitric oxide is fundamental to neurovascular coupling in humans. J Physiol 598, 4927–4939. [PubMed: 32785972]

Hoiland RL, Fisher JA & Ainslie PN (2019). Regulation of the Cerebral Circulation by Arterial Carbon Dioxide. Compr Physiol 9, 1101–1154. [PubMed: 31187899]

Hoiland RL, Tymko MM, Bain AR, Wildfong KW, Monteleone B & Ainslie PN (2016). Carbon dioxide-mediated vasomotion of extra-cranial cerebral arteries in humans: a role for prostaglandins? J Physiol 594, 3463–3481. [PubMed: 26880615]

Hoscheidt SM, Kellawan JM, Berman SE, Rivera-Rivera LA, Krause RA, Oh JM, Beeri MS, Rowley HA, Wieben O, Carlsson CM, Asthana S, Johnson SC, Schrage WG & Bendlin BB (2017). Insulin resistance is associated with lower arterial blood flow and reduced cortical perfusion in cognitively asymptomatic middle-aged adults. J Cereb Blood Flow Metab 37, 2249–2261. [PubMed: 27488909]

Ide K, Worthley M, Anderson T & Poulin MJ (2007). Effects of the nitric oxide synthase inhibitor L -NMMA on cerebrovascular and cardiovascular responses to hypoxia and hypercapnia in humans: Effects of L -NMMA on CBF responses to alterations in blood gases. The Journal of Physiology 584, 321–332. [PubMed: 17673507]

Ilkka H, Bengt S, Jukka K, Sipilä HT, Vesa O, Pirjo N, Juhani K, Kari K & Ylva H (2011). Skeletal muscle blood flow and oxygen uptake at rest and during exercise in humans: a pet study with nitric oxide and cyclooxygenase inhibition. American Journal of Physiology-Heart and Circulatory Physiology 300, H1510–H1517. [PubMed: 21257921]

Imig JD, Gebremedhin D, Harder DR & Roman RJ (1993). Modulation of vascular tone in renal microcirculation by erythrocytes: role of EDRF. American Journal of Physiology-Heart and Circulatory Physiology 264, H190–H195.

Iordanova B, Li L, Clark RSB & Manole MD (2017). Alterations in Cerebral Blood Flow after Resuscitation from Cardiac Arrest. Front Pediatr 5, 174. [PubMed: 28861407]

Jiang J, Zheng J-P, Li Y, Gan Z, Jiang Y, Huang D, Li H, Liu Z & Ke Y (2016). Differential contribution of endothelium-derived relaxing factors to vascular reactivity in conduit and resistance arteries from normotensive and hypertensive rats. Clinical and Experimental Hypertension 38, 393–398. [PubMed: 27159544]

Johnson KM, Lum DP, Turski PA, Block WF, Mistretta CA & Wieben O (2008). Improved 3D phase contrast MRI with off-resonance corrected dual echo VIPR: Improved 3D PC MRI With Corrected Dual Echo VIPR. Magn Reson Med 60, 1329–1336. [PubMed: 19025882]

Johnson NA, Jahng G-H, Weiner MW, Miller BL, Chui HC, Jagust WJ, Gorno-Tempini ML & Schuff N (2005). Pattern of Cerebral Hypoperfusion in Alzheimer Disease and Mild Cognitive Impairment Measured with Arterial Spin-labeling MR Imaging: Initial Experience. Radiology 234, 851–859. [PubMed: 15734937]

Joshi S, Young WL, Duong DH, Ostapkovich ND, Aagaard BD, Hashimoto T & Pile-Spellman J (2000). Intracarotid Infusion of the Nitric Oxide Synthase Inhibitor, l-NMMA, Modestly Decreases Cerebral Blood Flow in Human Subjects. Anesthesiology 93, 699–707. [PubMed: 10969303]

Author Manuscript Author Manuscript Author Manuscript Author Manuscript

Kamper AM, Spilt A, de Craen AJM, van Buchem MA, Westendorp RGJ & Blauw GJ (2004). Basal cerebral blood flow is dependent on the nitric oxide pathway in elderly but not in young healthy men. Experimental Gerontology 39, 1245–1248. [PubMed: 15288698]

Kellawan JM, Harrell JW, Schrauben EM, Hoffman CA, Roldan-Alzate A, Schrage WG & Wieben O (2016). Quantitative cerebrovascular 4D flow MRI at rest and during hypercapnia challenge. Magnetic Resonance Imaging 34, 422–428. [PubMed: 26708027]

Kellawan JM, Harrell JW, Roldan-Alzate A, Wieben O & Schrage WG (2017). Regional hypoxic cerebral vasodilation facilitated by diameter changes primarily in anterior versus posterior circulation. J Cereb Blood Flow Metab 37, 2025–2034. [PubMed: 27406213]

Kellawan JM, Peltonen GL, Harrell JW, Roldan-Alzate A, Wieben O & Schrage WG (2020). Differential contribution of cyclooxygenase to basal cerebral blood flow and hypoxic cerebral vasodilation. American Journal of Physiology-Regulatory, Integrative and Comparative Physiology 318, R468–R479.

Kiss B, Dallinger S, Findl O, Rainer G, Eichler H-G & Schmetterer L (1999). Acetazolamide-induced cerebral and ocular vasodilation in humans is independent of nitric oxide. American Journal of Physiology-Regulatory, Integrative and Comparative Physiology 276, R1661–R1667.

Kitagawa K, Oku N, Kimura Y, Yagita Y, Sakaguchi M, Hatazawa J & Sakoda S (2009). Relationship between cerebral blood flow and later cognitive decline in hypertensive patients with cerebral small vessel disease. Hypertens Res 32, 816–820. [PubMed: 19575014]

Kovách AG, Szabó C, Benyó Z, Csáki C, Greenberg JH & Reivich M (1992). Effects of NG-nitro-L-arginine and L-arginine on regional cerebral blood flow in the cat. The Journal of Physiology 449, 183–196. [PubMed: 1522509]

Lassen LH, Christiansen I, Iversen H, Jansen-Olesen I & Olesen J (2003). The Effect of Nitric Oxide Synthase Inhibition on Histamine Induced Headache and Arterial Dilatation in Migraineurs. Cephalalgia 23, 877–886. [PubMed: 14616929]

Lassen LH, Klingenberg Iversen H & Olesen J (2003). A dose-response study of nitric oxide synthase inhibition in different vascular beds in man. European Journal of Clinical Pharmacology 59, 499–505. [PubMed: 13680036]

Lassen LH, Sperling B, Andersen A & Olesen J (2005). The effect of I.V. L-N ^{G} Methylarginine Hydrochloride (L-NMMA: 546C88) on Basal and Acetazolamide (Diamox®) induced Changes of Blood Velocity in Cerebral Arteries and Regional Cerebral Blood flow in Man. Cephalalgia 25, 344–352. [PubMed: 15839849]

Lee C, Lopez OL, Becker JT, Raji C, Dai W, Kuller LH & Gach HM (2009). Imaging Cerebral Blood Flow in the Cognitively Normal Aging Brain with Arterial Spin Labeling: Implications for Imaging of Neurodegenerative Disease. Journal of Neuroimaging 19, 344–352. [PubMed: 19292827]

Leeuwis AE, Benedictus MR, Kuijer JPA, Binnewijzend MAA, Hooghiemstra AM, Verfaillie SCJ, Koene T, Scheltens P, Barkhof F, Prins ND & van der Flier WM (2017). Lower cerebral blood flow is associated with impairment in multiple cognitive domains in Alzheimer's disease. Alzheimer's & Dementia 13, 531–540.

Leeuwis AE, Hooghiemstra AM, Bron EE, Kuipers S, Oudeman EA, Kalay T, Brunner-La Rocca H, Kappelle LJ, Oostenbrugge RJ, Greving JP, Niessen WJ, Buchem MA, Osch MJP, Rossum AC, Prins ND, Biessels G, Barkhof F, Heart–Brain Connection consortium & der Flier WM (2020). Cerebral blood flow and cognitive functioning in patients with disorders along the heart–brain axis: Cerebral blood flow and the heart–brain axis. Alzheimer's & Dementia: Translational Research & Clinical Interventions; DOI: 10.1002/trc2.12034.

Lefroy DC, Crake T, Uren NG, Davies GJ & Maseri A (n.d.). Effect of inhibition of nitric oxide synthesis on epicardial coronary artery caliber and coronary blood flow in humans. 12.

Lewis NCS, Bain AR, MacLeod DB, Wildfong KW, Smith KJ, Willie CK, Sanders ML, Numan T, Morrison SA, Foster GE, Stewart JM & Ainslie PN (2014). Impact of hypocapnia and cerebral perfusion on orthostatic tolerance. The Journal of Physiology 592, 5203–5219. [PubMed: 25217373]

Liu P, Smith PF, Appleton I, Darlington CL & Bilkey DK (2003). Nitric oxide synthase and arginase in the rat hippocampus and the entorhinal, perirhinal, postrhinal, and temporal cortices: Regional variations and age-related changes. Hippocampus 13, 859–867. [PubMed: 14620881]

Author Manuscript Author Manuscript Author Manuscript Author Manuscript

Love S & Miners JS (2016). Cerebrovascular disease in ageing and Alzheimer's disease. Acta Neuropathol 131, 645–658. [PubMed: 26711459]

Luksha L, Agewall S & Kublickiene K (2009). Endothelium-derived hyperpolarizing factor in vascular physiology and cardiovascular disease. Atherosclerosis 202, 330–344. [PubMed: 18656197]

Markus HS, Vallance P & Brown MM (1994). Differential effect of three cyclooxygenase inhibitors on human cerebral blood flow velocity and carbon dioxide reactivity. Stroke 25, 1760–1764. [PubMed: 8073456]

Martin BJ, Yip B, Hearty M, Marietta S & Hill R (2002). Outcome, Functional Recovery and Unmet Needs following Acute Stroke. Experience of Patient follow up at 6 to 9 Months in a Newly Established Stroke Service. Scott Med J 47, 136–137. [PubMed: 12616970]

Muller M, van der Graaf Y, Visseren FL, Mali WPThM, Geerlings MI, & for the SMART Study Group (2012). Hypertension and longitudinal changes in cerebral blood flow: The SMART-MR study. Ann Neurol 71, 825–833. [PubMed: 22447734]

Northington FJ, Tobin JR, Harris AP, Traystman RJ & Koehler RC (1997). Developmental and Regional Differences in Nitric Oxide Synthase Activity and Blood Flow in the Sheep Brain. J Cereb Blood Flow Metab 17, 109–115. [PubMed: 8978393]

O'Brien JT, Erkinjuntti T, Reisberg B, Roman G, Sawada T, Pantoni L, Bowler JV, Ballard C, DeCarli C, Gorelick PB, Rockwood K, Burns A, Gauthier S & DeKosky ST (n.d.). Vascular cognitive impairment. 10.

Peltonen GL, Harrell JW, Aleckson BP, LaPlante KM, Crain MK & Schrage WG (2016). Cerebral blood flow regulation in women across menstrual phase: differential contribution of cyclooxygenase to basal, hypoxic, and hypercapnic vascular tone. American Journal of Physiology-Regulatory, Integrative and Comparative Physiology 311, R222–R231.

Peltonen GL, Harrell JW, Rousseau CL, Ernst BS, Marino ML, Crain MK & Schrage WG (2015). Cerebrovascular regulation in men and women: stimulus-specific role of cyclooxygenase. Physiol Rep 3, e12451. [PubMed: 26149282]

Pohjasvaara T, Erkinjuntti T, Ylikoski R, Hietanen M, Vataja R & Kaste M (1998). Clinical Determinants of Poststroke Dementia. Stroke 29, 75–81. [PubMed: 9445332]

Reitz C, Luchsinger JA & Mayeux R (2008). Vascular disease and cognitive impairment. Expert Review of Neurotherapeutics 8, 1171–1174. [PubMed: 18671658]

Rivera-Rivera LA, Turski P, Johnson KM, Hoffman C, Berman SE, Kilgas P, Rowley HA, Carlsson CM, Johnson SC & Wieben O (2016). 4D flow MRI for intracranial hemodynamics assessment in Alzheimer's disease. J Cereb Blood Flow Metab 36, 1718–1730. [PubMed: 26661239]

Rocha MP, Campos MO, Mattos JD, Mansur DE, Rocha HNM, Secher NH, Nóbrega ACL & Fernandes IA (2020). K_{ATP} channels modulate cerebral blood flow and oxygen delivery during isocapnic hypoxia in humans. J Physiol 598, 3343–3356. [PubMed: 32463117]

Roy B, Woo MA, Wang DJJ, Fonarow GC, Harper RM & Kumar R (2017). Reduced regional cerebral blood flow in patients with heart failure: Reduced regional cerebral blood flow in HF. Eur J Heart Fail 19, 1294–1302. [PubMed: 28560737]

Schrauben E, Wåhlin A, Ambarki K, Spaak E, Malm J, Wieben O & Eklund A (2015). Fast 4D flow MRI intracranial segmentation and quantification in tortuous arteries: Fast 4D Flow Processing Tool. J Magn Reson Imaging 42, 1458–1464. [PubMed: 25847621]

Shesely EG, Maeda N, Kim H-S, Desai KM, Krege JH, Laubach VE, Sherman PA, Sessa WC & Smithies O (1996). Elevated blood pressures in mice lacking endothelial nitric oxide synthase. Proceedings of the National Academy of Sciences 93, 13176–13181.

Shimokawa H, Yasutake H, Fujii K, Owada MK, Nakaike R, Fukumoto Y, Takayanagi T, Nagao T, Egashira K, Fujishima M & Takeshita A (1996). The Importance of the Hyperpolarizing Mechanism Increases as the Vessel Size Decreases in Endothelium-Dependent Relaxations in Rat Mesenteric Circulation: Journal of Cardiovascular Pharmacology 28, 703–711. [PubMed: 8945685]

Urakami-Harasawa L, Shimokawa H, Nakashima M, Egashira K & Takeshita A (1997). Importance of endothelium-derived hyperpolarizing factor in human arteries. J Clin Invest 100, 2793–2799. [PubMed: 9389744]

Author Manuscript Author Manuscript Author Manuscript Author Manuscript

Van Mil AHM, Spilt A, Van Buchem MA, Bollen ELEM, Teppema L, Westendorp RGJ & Blauw GJ (2002). Nitric oxide mediates hypoxia-induced cerebral vasodilation in humans. Journal of Applied Physiology 92, 962–966. [PubMed: 11842027]

Vikner T, Nyberg L, Holmgren M, Malm J, Eklund A & Wåhlin A (2020). Characterizing pulsatility in distal cerebral arteries using 4D flow MRI. J Cereb Blood Flow Metab 40, 2429–2440. [PubMed: 31722598]

Wagner M, Jurcoane A, Volz S, Magerkurth J, Zanella FE, Neumann-Haefelin T, Deichmann R, Singer OC & Hattingen E (2012). Age-Related Changes of Cerebral Autoregulation: New Insights with Quantitative T2′-Mapping and Pulsed Arterial Spin-Labeling MR Imaging. AJNR Am J Neuroradiol 33, 2081–2087. [PubMed: 22700750]

Wen B, Tian S, Cheng J, Li Y, Zhang H, Xue K, Zhang Z, Fan Y & Wu B (2019). Test–retest multisite reproducibility of neurovascular 4D flow MRI. J Magn Reson Imaging 49, 1543–1552. [PubMed: 30443945]

White RP, Deane C, Vallance P & Markus HS (1998). Nitric Oxide Synthase Inhibition in Humans Reduces Cerebral Blood Flow but Not the Hyperemic Response to Hypercapnia. Stroke 29, 467–472. [PubMed: 9472891]

White RP, Hindley C, Bloomfield PM, Cunningham VJ, Vallance P, Brooks DJ & Markus HS (1999). The Effect of the Nitric Oxide Synthase Inhibitor L-NMMA on Basal CBF and Vasoneuronal Coupling in Man: A PET Study. J Cereb Blood Flow Metab 19, 673–678. [PubMed: 10366198]

Willie CK, Tzeng Y-C, Fisher JA & Ainslie PN (2014). Integrative regulation of human brain blood flow: Integrative regulation of human brain blood flow. The Journal of Physiology 592, 841–859. [PubMed: 24396059]

Wolters FJ, Zonneveld HI, Hofman A, van der Lugt A, Koudstaal PJ, Vernooij MW & Ikram MA (2017). Cerebral Perfusion and the Risk of Dementia: A Population-Based Study. Circulation 136, 719–728 [PubMed: 28588075]

Author Manuscript Author Manuscript Author Manuscript Author Manuscript

Key points summary

- Cerebral blood flow (CBF) is vital for brain health, but the signals key to regulating CBF remain unclear.
- Nitric oxide (NO) is produced in the brain, but its importance in regulating CBF remains controversial since prior studies have not studied all regions of the brain simultaneously.
- Using modern MRI approaches, a drug that inhibits enzymes that make NO (L-NMMA) reduced CBF up to 11% in different brain regions.
- NO helps maintain proper CBF in healthy adults. These data will help us understand if reductions in CBF which occur during aging or cardiovascular disease are related to shifts in NO signaling.

Author Manuscript Author Manuscript Author Manuscript Author Manuscript

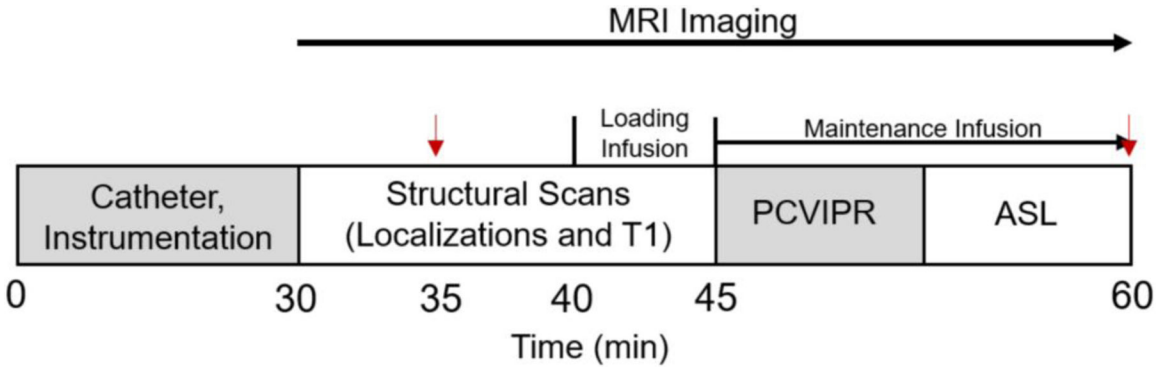

Figure 1: Experimental protocol timeline.

Participants reported to the MRI, and an IV catheter was placed in one arm for drug infusion. Participants then underwent MRI imaging for ~30 minutes. Structural scans included localizations and a T1-weighted image for ASL co-registration. Drug infusion occurred over the last 5 minutes of structural scanning, and then PCVIPR and ASL images were then taken. Vertical arrows (↓) indicate where blood pressure and hemodynamics (HR, SpO_2, $ETCO_2$) were measured.

Author Manuscript Author Manuscript Author Manuscript Author Manuscript

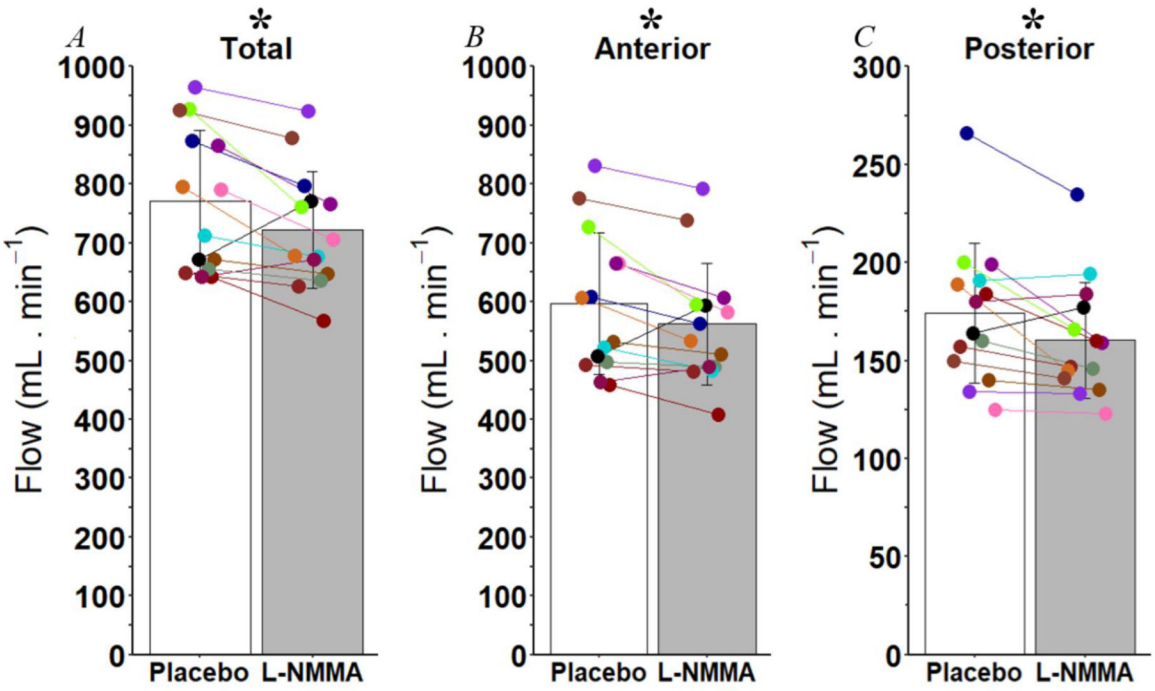

Figure 2: Total and regional cerebral blood flow.

Statistical comparison was made using a paired T-test or Wilcox test if appropriate, n = 14. A, Total cerebral blood flow (CBF) was calculated as: $CBF_{R\text{-}ICA}$ + $CBF_{L\text{-}ICA}$ + CBF_{BA}. B, Anterior CBF was calculated as: $CBF_{R\text{-}ICA}$ + $CBF_{L\text{-}ICA}$. C, Posterior CBF was defined as CBF_{BA}. The asterisk (*) symbol indicates a significant difference in the CBF response between placebo and L-NMMA trials, $P \leq 0.05$.

Author Manuscript Author Manuscript Author Manuscript Author Manuscript

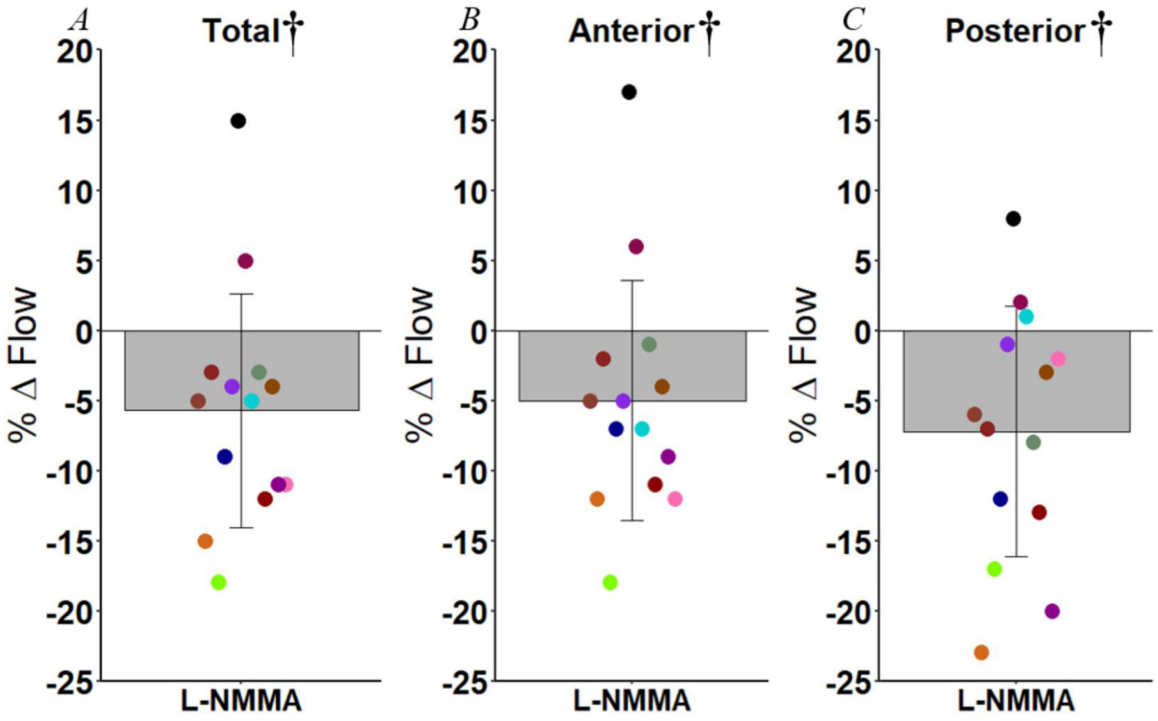

Figure 3: %Δ Total and regional cerebral blood flow.

Statistical comparison was made using a paired one-way T-test or Wilcox test if appropriate, n = 14. A, %Δ total flow. B, %Δ anterior flow. C, %Δ posterior flow. The dagger (†) symbol indicates a significant effect of L-NMMA that is different than 0.

Author Manuscript Author Manuscript Author Manuscript Author Manuscript

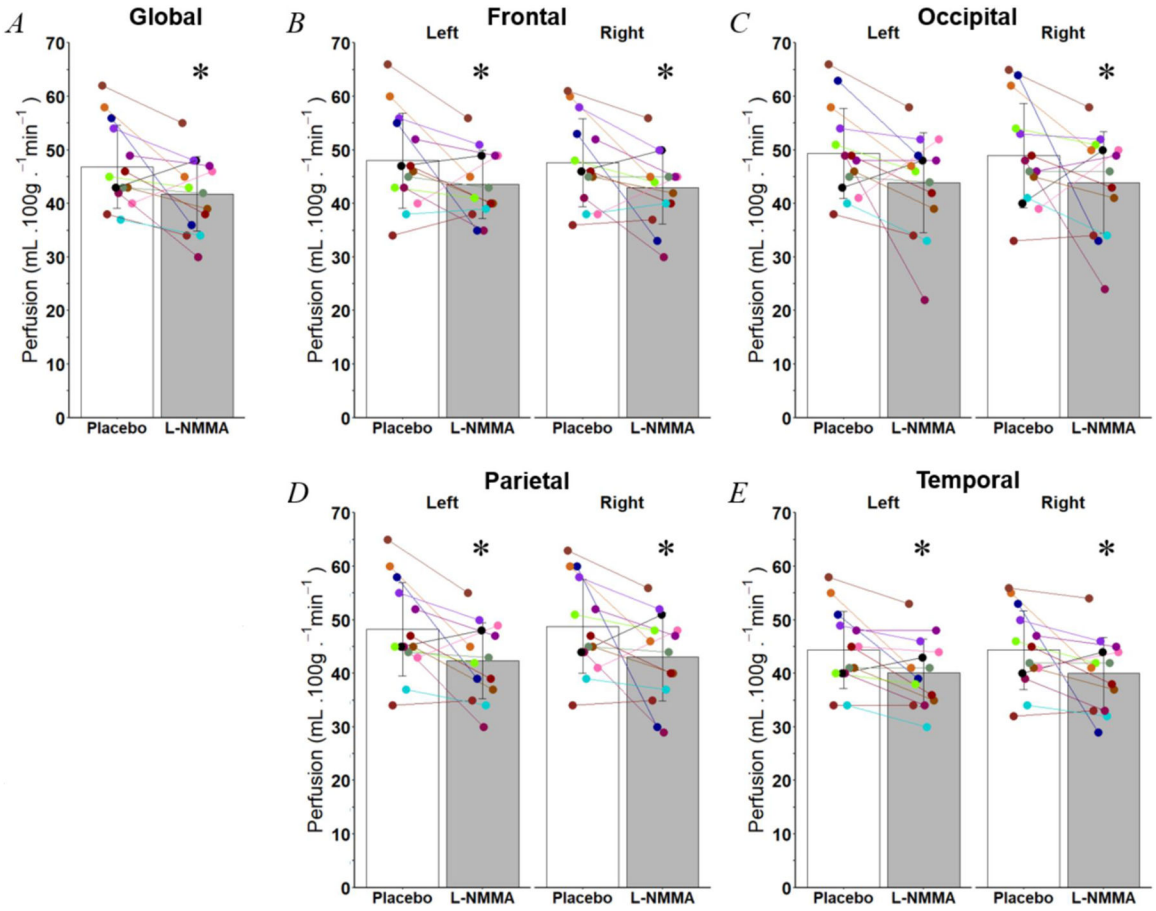

Figure 4: Global and regional perfusion with placebo and L-NMMA infusions.

Statistical comparison was made using a paired T-test or Wilcox test if appropriate, n=14. A, global perfusion. B, left and right frontal lobe perfusion. C, left and right occipital lobe perfusion. D, left and right parietal lobe perfusion. E, left and right temporal lobe perfusion The asterisk (*) symbol indicates a significant difference between placebo and L-NMMA trials, $P \leq 0.05$.

Author Manuscript

Author Manuscript

Author Manuscript

Author Manuscript

Table 1.

Subject characteristics

n	**14 (7 Male, 7 Female)**
Age, yr	24 ± 5
Height, cm	172 ± 8
Weight, kg	65 ± 8
BMI, kg/m^2	22 ± 2
Waist, cm	74 ± 6
Hip, cm	96 ± 6
Glucose, mg/dL	84 ± 17
Total cholesterol, mg/dL	146 ± 37
HDL, mg/dL	71 ± 18
LDL, mg/dL	67 ± 20
Triglycerides, mg/dL	71 ± 19
SBP, mmHg	112 ± 8
DBP, mmHg	69 ± 5
MABP, mmHg	83 ± 7

Values are means ± SD. BMI, body mass index; DBP, diastolic blood pressure; HDL, high density lipoprotein; LDL, low density lipoprotein; MABP, mean arterial blood pressure; SBP, systolic blood pressure.

Author Manuscript

Author Manuscript

Author Manuscript

Author Manuscript

Table 2.

Systemic hemodynamics at baseline and post-MRI scanning

	Placebo	L-NMMA
Heart rate, beats/min		
Baseline	59 ± 8	57 ± 7
Post-Drug Infusion	55 ± 5‡	49 ± 6‡
Post-Scan	62 ± 10§	56 ± 6§
SBP, mmHg		
Baseline	114 ± 10	113 ± 7
Post-Scan	114 ± 9	116 ± 7*
DBP, mmHg		
Baseline	67 ± 8	63 ± 6
Post-Scan	65 ± 10	66 ± 9*
MABP, mmHg		
Baseline	88 ± 8	85 ± 7
Post-Scan	86 ± 10	89 ± 8*
$ETCO_2$, mmHg		
Baseline	36 ± 3	36 ± 3
Post-Scan	35 ± 4	35 ± 3

Values are presented as means ± SD, n = 14 except for $ETCO_2$ (range is n = 9–13); see discussion. DBP, diastolic blood pressure; $ETCO_2$, end-tidal carbon dioxide; MABP, mean arterial blood pressure; SBP, systolic blood pressure. The double dagger (‡) symbol indicates a difference between baseline and post-drug infusion within a condition; the section sign (§) symbol indicates a difference between post-drug infusion and post-scan within a condition; the asterisk (*) symbol indicates a difference between baseline and post-scan within a condition. Significance was set at $P \leq 0.017$ for heart rate, $P \leq 0.05$ for $ETCO_2$, and $P \leq 0.025$ for all other measures.

Author Manuscript

Author Manuscript

Author Manuscript

Author Manuscript

Table 3.

Basal cerebral blood flow under placebo and L-NMMA conditions

	Total	Anterior	Posterior
Flow, mL/min			
Placebo	771 ± 121	597 ± 121	174 ± 36
L-NMMA	722 ± 100*	562 ± 103*	160 ± 30*
ΔFlow, mL/min			
L-NMMA	−49 ± 64†	−35 ± 51†	−14 ± 18†
%ΔFlow			
L-NMMA	−6 ± 8†	−5 ± 9†	−7 ± 9†

Values are presented as means ± SD, n = 14. The asterisk (*) symbol indicates a significant difference in the CBF response between from placebo and L-NMMA trials. The dagger (†) symbol indicates a significant basal effect of NOS inhibition. $P \leq 0.05$.

Author Manuscript Author Manuscript Author Manuscript Author Manuscript

Table 4.

Vessel-specific cerebrovascular responses with L-NMMA vs. placebo

	ICA		MCA		ACA		VA			PCA	
	Left	**Right**	**Left**	**Right**	**Left**	**Right**	**Left**	**Right**	**BA**	**Left**	**Right**
n, Placebo	14	14	13	12	12	14	13	12	14	13	14
n, L-NMMA	14	14	12	12	12	14	13	12	14	13	14
Flow, mL/min											
Placebo	286±69	311±69	186±17	172±20	101±25	110±37	108±40	109±39	174±36	76±11	74±12
L-NMMA	*274±63**	288±62*	179±24	170±25	99±30	104±36	*102±38**	102± 6*	160±30*	*71±11**	73±14
ΔFlow, mL/min											
L-NMMA	*−12±21†*	−23±31†	−2±17	−1±16	−1±14	−6 ±16	−5±13	−7±8†	−14±18†	*−6±10†*	−1±8
%ΔFlow											
L-NMMA	*−4±7†*	−7±11†	−1±9	−1±10	−2±14	−4±21	−5±13	−6±8†	−7±9†	−6±14	−1±11
CSA, mm^2											
Placebo	15.4±3.2	16.2 ±3.0	7.4±1.3	7.3±1.1	5.7±0.7	6.0±1.2	6.6±0.7	6.9±1.4	8.9±1.4	5.2±0.7	5.3±0.7
L-NMMA	14.9±3.0	*15.2±3.0**	6.9±0.8*	*6.9±0.9**	5.3±0.8*	5.3±0.8*	6.2±0.8*	6.5±1.0*	8.5±1.4*	4.9±0.5	*4.9±0.4**
ΔCSA, mm^2											
L-NMMA	−0.5±1.5	*−0.9±1.9†*	−0.6±1.0†	*−0.4±0.6†*	−0.4±0.5†	−0.7±0.9†	−0.4±0.5†	−0.4±0.7†	−0.4±0.7†	−0.4±0.8	−0.4±0.8
%ΔCSA											
L-NMMA	−3±9	−5±11	−6±10†	*−5±7†*	−7±8†	−10±12†	−6±7†	−5±7†	−4±7†	−6±12	−6±13
Mean velocity, cm/s											
Placebo	31±5	32±5	43±8	40±5	29±6	31±7	27±8	25±6	33±5	25±4	24±5
L-NMMA	31±6	32±6	44±7	41±6	31±7	32±7	27±7	25±7	32±5	24±4	25±5
ΔMean velocity, cm/s											
L-NMMA	0±4	0±4	2±6	2±5	2±3	2±5	0±3	0±2	−1±3	0±4	1±4
%ΔMean velocity											
L-NMMA	0±12	−1±11	7±19	4±12	6±12	8±20	2±11	−1±9	−3±9	1±16	7±22

Statistical comparison was made using a paired T-test or Wilcox test if appropriate. Values are presented as means ± SD. ACA, anterior cerebral artery; BA, basilar artery; CSA, cross-sectional area; ICA, internal carotid artery; MCA, middle cerebral artery; PCA, posterior cerebral artery; VA, vertebral artery. The asterisk (*) symbol indicates a significant difference between placebo and L-NMMA trials, P ≤ 0.05. The dagger (†) symbol indicates a significant effect of L-NMMA that is different than 0. Italics indicate results that change from significant to trending ($p<0.1$) when the female studied outside of follicular days 1–5 was removed from the analysis.

J Physiol. Author manuscript; available in PMC 2022 November 01.

Author Manuscript Author Manuscript Author Manuscript Author Manuscript

Table 5.

Global and regional cerebral perfusion

		Frontal		Occipital		Parietal		Temporal	
	Global	**Left**	**Right**	**Left**	**Right**	**Left**	**Right**	**Left**	**Right**
Flow, mL · 100g^{-1} · min^{-1}									
Placebo	47±8	48±9	48±8	49±8	49±10	48±9	49±9	44±7	44±7
L-NMMA	42±7*	44±6*	43±7*	44±9*	44±10	42±7*	43±8*	40±6*	40±7*
ΔFlow									
L-NMMA	−5±7†	−4±8†	−5±7†	−5±9†	*−5±11*	−6±7†	−6±9†	−4±5†	−5±7†
%ΔFlow									
L-NMMA	−10±14†	*−7±15†*	−9±15†	−10±18†	−8±22	−11±14†	−10±17†	−9±10†	−9±14†

Statistical comparison was made using a paired T-test or Wilcox test if appropriate. Values are presented as means ± SD, n = 14. The asterisk (*) symbol indicates a significant difference between placebo and L-NMMA trials, P ≤ 0.05. The dagger (†) symbol indicates a significant effect of L-NMMA that is different than 0. Italics indicate results that changed from significant to trending (%ΔCBF for left frontal lobe, p=0.054) or trending to significant (ΔCBF for right occipital lobe, p = 0.047) when the female studied outside of follicular days 1–5 was removed from the analysis.

J Physiol. Author manuscript; available in PMC 2022 November 01.

Author Manuscript Author Manuscript Author Manuscript Author Manuscript

Table 6.

Cerebral perfusion through the major vascular territories

	Pooled	ACA Territory		MCA Territory		PCA Territory	
	Territories	Left	Right	Left	Right	Left	Right
Flow, mL · 100g^{-1} · min^{-1}							
Placebo	47 ± 8	50 ± 9	50 ± 10	46 ± 8	47 ± 8	47 ± 8	47 ± 9
L-NMMA	41 ± 7*	44 ± 8*	44 ± 8*	41 ± 6*	42 ± 8*	42 ± 9*	41 ± 9*
ΔFlow							
L-NMMA	−5 ± 7†	−6 ± 8†	−5 ± 9†	−5 ± 6†	−5 ± 8†	−5 ± 8†	−6 ± 11†
%ΔFlow							
L-NMMA	−10 ± 14†	−10 ± 15†	−9 ± 16†	−9 ± 13†	−9 ± 16†	−9 ± 19	−10 ± 22

Statistical comparison was made using a paired T-test or Wilcox test if appropriate. Values are presented as means ± SD, n = 13. The asterisk (*) symbol indicates a significant difference between placebo and L-NMMA trials, P ≤ 0.05. The dagger (†) symbol indicates a significant effect of L-NMMA that is different than 0.

J Physiol. Author manuscript; available in PMC 2022 November 01.